Published in IET Microwaves, Antennas & Propagation
Received on 17th July 2008
Revised on 14th November 2008
doi: 10.1049/iet-map.2008.0234

ISSN 1751-8725

Three-dimensional antennas array for the estimation of direction of arrival

F. Harabi[1] *A. Gharsallah*[1] *S. Marcos*[2]

[1]*Faculty of Sciences, El Manar 2092, Tunisia*
[2]*Laboratory of Signals and Systems (L2S), The National Scientific Research Center, Electric Superior School, Paris, France*
E-mail: feridsamia@yahoo.fr

Abstract: Direction of arrival (DOA) estimation of multiple sources using an antenna array becomes very important in wireless communications. It is well known that the quality of the DOA estimation depends on the selected technique and algorithm but it also depends on the geometrical configuration of the antenna array used during the estimation. The authors study the influence of the antenna array configurations on the Cramer–Rao bounds (CRB) of the 2D DOA estimation problem as well as on the performance of the well known MUSIC algorithm. For this we consider the most known planar arrays and we propose a 2-L shaped 3D antennas array. It appears that this 3D antennas array outperforms the other configurations as well as that already proposed in Tayem and Kwon (2005), in terms of both the CRB and the MUSIC root mean square estimation error and also removes ambiguities from the estimation MUSIC pseudo spectrum.

1 Introduction

Direction of arrival (DOA) estimation has been an intensively investigated topic in signal processing for some decades. A large number of DOA algorithms have been studied and developed from the beam-former methods [1] to the high resolution methods like MUSIC [2], ESPRIT [3, 4] and their variations and the maximum likelihood methods [5–8]. In [9], the authors provided an excellent review and comparison of the various narrowband techniques. Despite this large literature, limited research has considered the impact of the array geometrical configuration on the quality of the DOA estimation.

The uniform linear array (ULA) has been applied in many works to estimate the 1D (azimuth only) DOA [10–13]. But, for the 2D (azimuth and elevation) DOA estimation problem, at least a planar array is required.

Liang and Paulraj [14] performed computer simulations to compare the diversity performance of several planar array configurations in a multi-path channel. For all the compared arrays, the difference between configurations decreased with an increasing multi-path angle spread and an increasing number of elements.

The Cramer–Rao bound (CRB) is widely used to evaluate the ultimate attainable performance in an estimation problem. It serves as an important tool in the performance evaluation of estimators involved in the field of communications and signal processing. In [15] a CRB analysis of the planar and 3D arrays was presented and several designs of isotropic planar and volume arrays were studied. In [16], Gazzah and Marcos have presented a simplified CRB expression for the study of the geometry impact of planar antenna array on the accuracy of the estimated DOA of single source. The authors have also taken into consideration the array ambiguity problem. Other studies of the performance of some planar array geometries are given in [17–19].

In this paper, we study the impacts of antenna array geometries on the performance of DOA estimation by computing the expression of the CRB for the circular, rectangular and L-shaped antenna arrays and compare them with those of a 3D antenna array configured as a 2-L shaped array.

The idea of using L-shaped arrays is not new, for example [20] and [21]. But the elements of the L-shaped array in our paper are placed in the $x-y$ axes whereas the elements in [20] are placed in the $x-z$. In [21], Maohui presents the

advantages of using the L-shaped array in comparison with the uniform circular array (UCA) for the 2D DOA estimation problem and shows that the L-shaped array not only has a simpler array manifold but also yields a smaller estimation error.

In [20] the authors proposed the 2-L shaped array for the estimation of both the elevation and the azimuth angles. They decomposed the antenna array in three linear uniform sub-arrays and brought the problem back to a one dimension problem by estimating independently the elevation angle by the sub-array placed on the z-axis and the azimuth angle by the sub-arrays placed on the x-axis and the y-axis. In this paper, we propose to deal with the 3D case by considering the entire 2-L shaped antenna array and jointly estimating the elevation and azimuth angles.

The improved performance of the MUSIC algorithm when using the proposed 2-L shaped antenna array will be presented in terms of root mean square estimation error (RMSE) of the estimated 2D DOA. In addition, the rate of detection of the DOAs using the different geometries of antenna arrays will be considered.

The rest of the paper is organised as follows. In Section 2 the antenna arrays manifold representation and the mathematical models used in this work are presented and a short review of the MUSIC algorithm used in simulations is given. In Section 3, we compute the CRBs for the estimation of the elevation and azimuth angles for each studied antenna array configuration. Section 4 presents simulation results concerning the advantage of the proposed 2-L shaped antennas array compared with the other antennas array configurations. Section 5 draws the conclusions.

2 Model assumptions and array geometries

2.1 Data model

In the scenario shown in Fig. 1, K narrow-band signals transmitted from K far-field sources travel through a homogeneous isotropic fluid medium and impinge on an array of M identical isotropic antennas or sensors located at $\boldsymbol{r}_m$ for $m \in [1, M]$. Let us note $\vartheta_k = [\varphi_k, \theta_k]$ the DOA of the kth source, with elevation angle $\theta_k \in [-\pi/2, \pi/2]$ measured clockwise relatively to the z-axis and azimuth angle $\varphi_k \in [0, 2\pi]$ measured counterclockwise relatively to the x-axis in the $x-y$ plane.

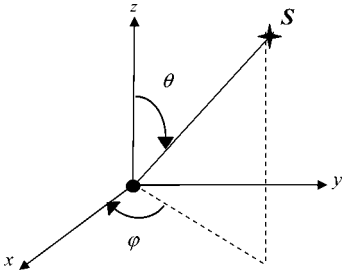

Figure 1 *3D system showing a signal arriving from azimuth φ and elevation θ*

The received signal is modelled as

$$\boldsymbol{x}(t) = \boldsymbol{A}(\varphi, \theta)\boldsymbol{s}(t) + \boldsymbol{n}(t) \quad (1)$$

where $\boldsymbol{x}(t)$ is the $M \times 1$ snapshot vector of the signals received simultaneously on all the sensors, $\boldsymbol{s}(t)$ is the $K \times 1$ vector of the source signals, $\boldsymbol{n}(t)$ is the $M \times 1$ noise vector that is assumed to be white, Gaussian and uncorrelated with the source signals. The $M \times K$ steering matrix $\boldsymbol{A}(\varphi, \theta) = [\boldsymbol{a}(\varphi_1, \theta_1), \ldots, \boldsymbol{a}(\varphi_K, \theta_K)]$ defines the array manifold and consists of the steering vectors $\boldsymbol{a}(\varphi_k, \theta_k)$ whose components are

$$a_m(\varphi_k, \theta_k) = \mathrm{e}^{j2\pi f \cdot \tau_m(\varphi_k, \theta_k)} \quad (2)$$

where $\tau_m(\varphi_k, \theta_k) = \boldsymbol{d}_k^{\mathrm{T}}(\varphi_k, \theta_k) \cdot \boldsymbol{r}_m / c$ is the propagation delay of source signal k received sensor m, c is the speed of propagation of the waves in the medium and $\boldsymbol{d}_k(\varphi_k, \theta_k)$ is the unit vector pointing towards source k.

In the 3D case, when the signal arrives from azimuth angle φ and elevation angle θ (see Fig. 1)

$$\boldsymbol{d}(\varphi, \theta) = [\cos(\varphi)\sin(\theta),\ \sin(\varphi)\sin(\theta),\ \cos(\theta)] \quad (3)$$

$\boldsymbol{r}_m = [x_m, y_m, z_m]^{\mathrm{T}}$ is the position vector of sensor m that depends on the geometry of the antenna array. In this paper, the circular, rectangular and L-shaped arrays shown in Fig. 2 will be addressed and compared to a 3D array with a 2-L shaped configuration.

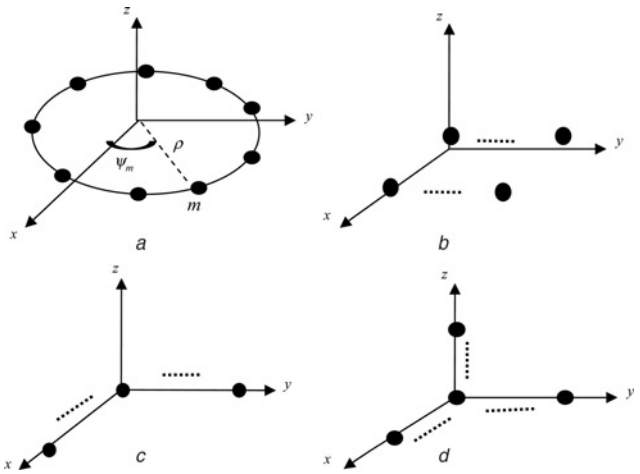

Figure 2 *Geometrical configurations of antennas array used in simulation, respectively*

a The circular array
b Rectangular array
c L-shaped array
d The 2-L shape array

IET Microw. Antennas Propag., 2009, Vol. 3, Iss. 5, pp. 843–849
doi: 10.1049/iet-map.2008.0234

2.2 Planar Arrays

Fig. 2 shows the array configurations used in this paper. Fig. 2*a* is a UCA, with radius ρ allowing that the elements are spaced by half a wavelength. The position vector $\boldsymbol{r}_{\text{cir}.m}$, in this case, is expressed as

$$\boldsymbol{r}_{\text{cir}.m} = [\rho \cos \psi_m, \rho \sin \psi_m, 0]^{\text{T}} \tag{4}$$

and the propagation delay is then

$$\tau_{\text{cir}.m}(\varphi_k, \theta_k) = \frac{\rho \sin \theta_k \cos(\varphi_k - \psi_m)}{c} \tag{5}$$

The antenna array in Fig. 2*b* has a rectangular configuration composed by two ULAs placed in parallel on the $x-y$ plane. The inter-sensor distance d is taken to be half a wavelength of the signal waves. Then the position vector $\boldsymbol{r}_{\text{rect}.m}$ can be expressed as

$$r_{\text{rect}.m} = [x_m, y_m, 0]^{\text{T}} \tag{6}$$

The propagation delay for the kth source on the mth sensor is derived as

$$\tau_{\text{rect}.m}(\varphi_k, \theta_k) = \frac{\sin \theta_k [x_m \cos(\varphi_k) + y_m \sin(\varphi_m)]}{c} \tag{7}$$

In the same way the L-shaped array presented in Fig. 1*c* is a particular case of planar antenna. The sensors are placed on the x and y axes. The sensors on the x axis have y and z co-ordinates equal to zero and the sensors on y axis have x and z co-ordinates equal to zero. The propagation delay of the kth source received on the mth element of the L-shaped array can also be determined from (7) using the proper co-ordinates.

2.3 3D array

In Fig. 2*d*, the 3D 2-L shaped array composed of three uniform linear sub-arrays placed on the x, y and z axes with inter-element spacing equal to d is presented. The element placed at the origin is common for referencing purposes. This antenna array configuration has already been proposed in [21] for the estimation of the 2D directions of arrival. However, the authors of [21] estimated independently the elevation angle by the sub-array placed on the z axis and the azimuth angle by both the sub-arrays placed on the x axis and the y axis. Here the investigation of the antennas array shape is different. Indeed, we here propose to jointly estimate the elevation and azimuth angles directly from the 3D 2-L shaped antenna array.

The position vector of the m-th element is expressed as

$$\boldsymbol{r}_{\text{2L}.m} = [x_m, y_m, z_m]^{\text{T}} \tag{8}$$

Then the propagation delay for the kth source on the mth sensor is derived as

$$\tau_{\text{2L}.m}(\varphi_k, \theta_k) = \frac{[x_m \cos(\varphi_k) \sin \theta_k + y_m \sin(\varphi_m) \sin \theta_k + z_m \cos(\theta_k)]}{c} \tag{9}$$

2.4 MUSIC algorithm

In order to compare the influence of the antenna array geometry of the 2D DOA estimation problem, we will consider the well-known MUSIC algorithm [2].

The correlation matrix of the sensor observations $\boldsymbol{x}(t)$ is

$$\boldsymbol{R} = E[\boldsymbol{x}(t) \cdot \boldsymbol{x}(t)^{\text{H}}] \tag{10}$$

where H represents a conjugate transposition. In practice, only a sample covariance matrix is available, that is, an estimate of $\boldsymbol{R}$ based on a finite number (P) of data samples or snapshots

$$\hat{\boldsymbol{R}} = \frac{1}{P} \sum_{j=1}^{P} x(t_j) \cdot x(t_j)^{\text{H}} \tag{11}$$

MUSIC algorithm relies on the eigenvalue decomposition of the correlation matrix $\hat{\boldsymbol{R}} = \boldsymbol{V} \Lambda \boldsymbol{V}^{\text{H}}$, where $\boldsymbol{V} = [\boldsymbol{v}_1, \ldots, \boldsymbol{v}_M]$, $\boldsymbol{\Lambda} = \text{diag}[\lambda_1, \ldots, \lambda_M]$, with $\boldsymbol{v}_k$ eigenvector (M-dimensional column vectors) and λ_k the eigenvalue associated with $\boldsymbol{v}_k$ sorted so as $\lambda_1 \geq \cdots \geq \lambda_K$. If the number K of sources is smaller than the number M of sensors, then all the signal components are represented in the signal subspace spanned by the first K eigenvectors $\boldsymbol{v}_1, \ldots, \boldsymbol{v}_K$, and the remaining $M-K$ eigenvectors $\boldsymbol{v}_{K+1}, \ldots, \boldsymbol{v}_M$ represent the noise subspace. The signal and the noise subspaces are orthogonal to each other.

The subspace spanned by the K steering vectors $\boldsymbol{a}(\varphi_1, \theta_1), \ldots, \boldsymbol{a}(\varphi_K, \theta_K)$ is also the signal subspace. When (φ, θ) coincides with one of the source 2D DOA $(\varphi_1, \theta_1), \ldots, (\varphi_K, \theta_K)$, the steering vector $\boldsymbol{a}(\varphi, \theta)$ and the noise subspace $\boldsymbol{v}_{K+1}, \ldots, \boldsymbol{v}_N$ are orthogonal, and therefore the so-called pseudo spectrum $U(\varphi, \theta) = \sum_{k=K+1}^{M} |\boldsymbol{v}_k^{\text{H}} \boldsymbol{a}(\varphi, \theta)|^2$ approaches zero. For the noise subspace to exist, the number M of sensors should be larger than the number K of sources. Thus, the MUSIC algorithm is applicable for mixtures of up to $M-1$ signals.

Note that some specific 2D DOA estimation algorithms have been developed in the literature in order to reduce the computational burden resulting in the search of zeros in a pseudo spectrum, see [22] and [23] for examples. However, the computational cost of the DOA estimation problem is not the topic of the present paper.

3 Cramer–Rao bounds

The CRB provide an unbeatable performance limit for any unbiased estimator and hence can be used to investigate the fundamental limits of parameter estimation problems or as a baseline for assessing the performance of a specific estimator. The CRB are also widely used in problems where the exact minimum-mean-square estimation error is difficult to evaluate. Indeed, the Cramer–Rao inequality [24] provides a relatively simple lower bound on the variance of unbiased estimators. For multi-parameter estimation, it has the form

$$\mathrm{var}(\hat{\theta}_i) \geq [\boldsymbol{J}^{-1}]_{ii}$$

where the ijth element of the Fisher information matrix $\boldsymbol{J}$ is given by

$$\boldsymbol{J}_{ij} = -\left[E\left\{\frac{\partial^2 \ln[p_{\boldsymbol{R}/\underline{\boldsymbol{\theta}}}(\boldsymbol{x}/\underline{\boldsymbol{\theta}})]}{\partial\theta_i \partial\theta_j}\right\}\right] \tag{12}$$

where $\underline{\boldsymbol{\theta}}$ is the parameter vector of components θ_i and θ_j to be estimated and $p_{\boldsymbol{R}/\underline{\boldsymbol{\theta}}}(\boldsymbol{x}/\underline{\boldsymbol{\theta}})$ is the probability density function of the observation vector $\boldsymbol{x}$ conditioned by $\underline{\boldsymbol{\theta}}$.

We are here interested by determining the CRB for each antenna array configuration seen previously and by analysing their characteristics. We address the problem of the joint estimation of the azimuth and elevation angles of a unique source. The CRB for the source DOA estimate is given by [15]

$$\mathrm{CRB}(\varphi, \theta) = [\boldsymbol{G}(\boldsymbol{B}, \varphi, \theta) \cdot T]^{-1} \tag{13}$$

where

$$T = \frac{2P(2\pi f M \sigma_s^2/c)^2}{\sigma_n^2(\sigma_n^2 + \sigma_s^2 M)} \tag{14}$$

$$\boldsymbol{G}(\boldsymbol{B}, \varphi, \theta) = \left[\frac{\partial \mathrm{d}(\varphi, \theta)}{\partial\varphi} \frac{\partial \mathrm{d}(\varphi, \theta)}{\partial\theta}\right]^{\mathrm{T}} \boldsymbol{B} \left[\frac{\partial \mathrm{d}(\varphi, \theta)}{\partial\varphi} \frac{\partial \mathrm{d}(\varphi, \theta)}{\partial\theta}\right] \tag{15}$$

$$\boldsymbol{B} = \frac{1}{M}\sum_{m=1}^{M} (\boldsymbol{r}_m - \boldsymbol{r}_c)(\boldsymbol{r}_m - \boldsymbol{r}_c)^{\mathrm{T}} \tag{16}$$

In (14), σ_s^2 and σ_n^2 are the signal and the noise variances, respectively. P is the number of snapshots and $\boldsymbol{r}_c$ in (16) is the centre of the array and expressed by

$$\boldsymbol{r}_c = \frac{1}{M}\sum_{m=1}^{M} \boldsymbol{r}_m \tag{17}$$

The CRB is the product of two terms. $\boldsymbol{G}(\boldsymbol{B}, \varphi, \theta)$ depends on the geometry of the antenna array through matrix $\boldsymbol{B}$, on the DOA (φ, θ) and on T that depends on the source and noise powers, the number of sensors and the number of snapshots. From the CRB expression, it appears that the only parameter that is going to change, according to the geometry of the antennas array, is the vector position $\boldsymbol{r}_m$.

4 Simulation results

Computer simulations have been conducted to evaluate the 2D DOA estimation performance of the considered antennas array configurations. Each antenna array contains eight isotropic sensors. The distance between two sensors is uniform and equal to half a wavelength of the source signal.

In Fig. 3, the CRB on the estimation of a single source DOA located at (20°, 70°) is presented for different array configurations. In fact, the mean of the azimuth angle CRB and the elevation angle CRB is plotted. Fig. 3*a* exhibits the CRB against the number of snapshots with an SNR = 0 dB and 8 sensors on each antenna array while Fig. 3*b* presents the CRB against SNR for 20 snapshots and 8 sensors. In both cases, the CRB obtained for the 2-L shaped array is lower than the CRB of the other configurations. This indicates that estimators using the 2-L shaped array may yield lower estimation errors than the one using the other antenna array geometries. It can also be

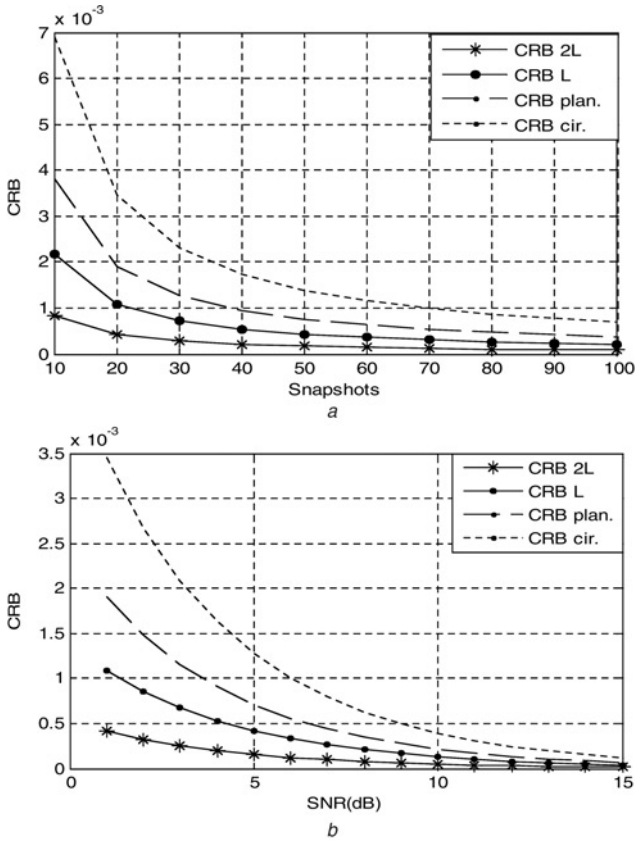

Figure 3 *CRBs for different antenna array geometries of eight sensors in the case of a source located at (20°, 70°)*

a Against snapshots with SNR = 0 dB
b Against SNR with 20 snapshots

doi: 10.1049/iet-map.2008.0234

noticed that among the planar antenna arrays above studied, the L shaped array has a lower CRB that the rectangular and circular arrays in the same conditions. This is in accordance with the results already obtained in [16].

Fig. 4 exhibits the pseudo spectrum $U(\varphi, \theta)$ of the MUSIC algorithm obtained for the different array configurations when jointly estimating the azimuth and elevation angles of a single source at (20°, 70°) with SNR = 0 dB and with 20 snapshots. It appears that only the 2-L shaped array gives an interesting result.

These results are generalised in Fig. 5 which exhibits the RMSE obtained by the MUSIC algorithm performed over 100 realisations and as a function of (a) the SNR for 20 snapshots and (b) the number of snapshots for SNR = 0 dB, respectively. The RMSE obtained with the 2-L shaped array is extensively lower than that of the other array configurations. This further shows the effectiveness of this 3D configuration.

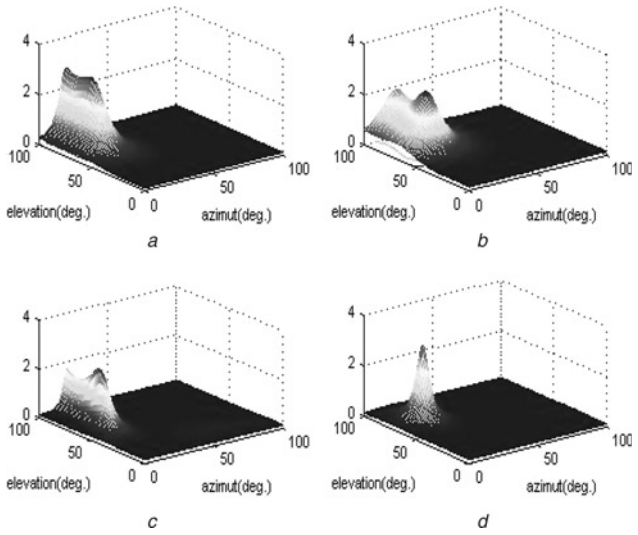

Figure 4 *Pseudo spectrum of MUSIC algorithm for the estimation of a single source located at (20°, 70°) with SNR = 0 dB, 20 snapshots and 8 elements in each array*

a Circular array
b Rectangular array
c L shaped array
d 2-L shaped array

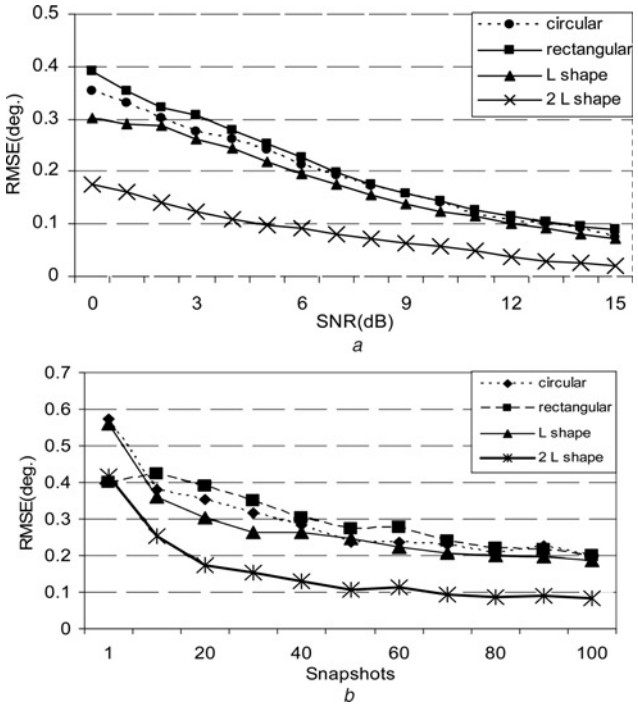

Figure 5 *RMSE of the DOA estimation of a single source located at (20°,70°) by MUSIC with 8 sensors in each array*

a According to the SNR with 20 snapshots
b According to snapshots with a SNR = 0 dB

Among the planar antenna arrays that are studied here, the L shaped array has a lower RMSE than the rectangular and circular arrays in the same conditions.

The study of the influence of the antenna array geometry on the detection of picks in the MUSIC pseudo spectrum yielding the elevation estimate is also presented as a function of the SNR and of the number of snapshots.

Tables 1 and 2 exhibit the rate of detection of picks in the MUSIC pseudo spectrum yielding the elevation estimate of a source located at (20°, 70°) for a total of 100 realisations, as a function of the SNR with 20 snapshots and as a function of the number of snapshots with a SNR = 0 dB, respectively.

In Table 1 the rate of detection of picks in the pseudo spectrum yielding to the estimation of the elevation angle by MUSIC algorithm with the 2-L shaped array attains

Table 1 Rate of detection of picks in the MUSIC pseudo spectrum yielding the elevation estimate for a source located at (20°, 70°) for different SNRs, 20 snapshots, 100 realisations and 8 sensors in each antenna array

SNR, dB	0	1	2	3	4	5	6	7	8	9	10
circular, %	83	87	91	94	98	100	100	100	100	100	100
rectangular, %	90	92	94	98	100	100	100	100	100	100	100
L shaped, %	80	87	94	97	100	100	100	100	100	100	100
2-L shaped, %	100	100	100	100	100	100	100	100	100	100	100

Table 2 Rate of detection of picks in the MUSIC pseudo spectrum yielding the elevation estimate for a source located at (20°, 70°) for different numbers of snapshots, SNR = 0 dB, 100 realisations and 8 sensors in each antenna array

Snapshots	1	10	20	30	40	50	60	70	80	90	100
circular, %	21	62	83	91	96	96	95	97	98	98	98
rectangular, %	29	69	90	96	98	99	99	99	100	100	100
L shaped, %	23	66	80	90	91	94	97	99	98	99	99
2-L shaped, %	60	94	100	100	100	100	100	100	100	100	100

100% at 0 dB. For the other planar arrays it attains 100% of detection at about 4 dB.

In Table 2 we observe that for only one observation, that is a difficult case to MUSIC algorithm and at 0 dB, the 2-L shaped antenna array allows to detect 60 times among 100 measures the picks in the pseudo spectrum yielding the estimated elevation angle. This proves again the efficiency of this array shape.

Let us now consider the case of the estimation of two close sources when using the different antenna array configurations. Fig. 6 exhibits the MUSIC pseudo spectra obtained in the presence of two sources located, at (20°, 70°) and (25°, 75°), respectively. Here SNR = 15 dB and 1000 snapshots are generated. The distinction of the two picks appears with the L-shaped antenna array and more clearly with the 2-L shaped antenna array. For the rectangular and circular antenna arrays the two picks are not clearly distinguished.

Finally, we present, in Fig. 7, the RMSE against SNR obtained by the MUSIC algorithm for the estimation of a single source located at (20°, 70°) when using the proposed 2-L shaped antenna array and the one proposed in [20] in the case of 20 snapshots and 8 elements (3 elements on the x axis sub-array, 2 elements on the z axis sub-array and 3 elements on the y axis sub-array). We observe that our proposed configuration and way of dealing with it can be about 4 dB better in SNR than the one used in [20].

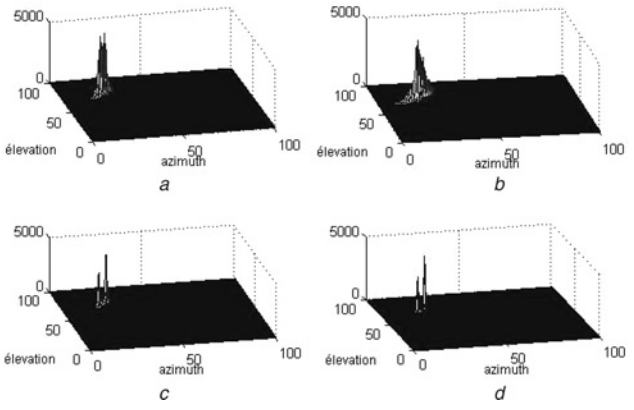

Figure 6 *3D pseudo spectra of the MUSIC algorithm for the estimation of two sources located at (20°, 70°) and (25°, 75°) for SNR = 15 dB and 1000 snapshots using 8 elements on each array*

a The circular array
b The rectangular array
c The L shaped array
d The 2-L shaped array

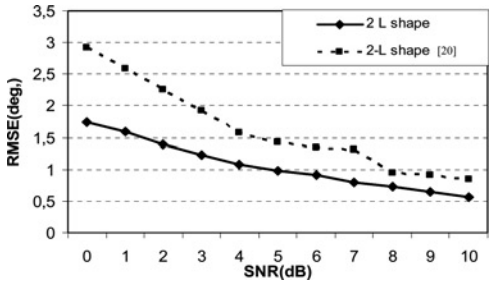

Figure 7 *RMSE against SNR obtained with the MUSIC algorithm for the estimation of a single source located at (20°, 70°) and 20 snapshots for the proposed 2-L shaped array and the one used in [20]*

5 Conclusion

In this paper, a comparative study of different planar antenna array configurations and a 3D 2-L shaped antenna array has been presented. For this, the CRBs have been compared. Also the accuracy of the joint azimuth and elevation estimation of a single source when using the MUSIC algorithm has been analysed for different antenna array configurations.

The 2-L shaped antenna array considered in this paper has a smaller CRB and exhibits a better RMSE when using the MUSIC algorithm and a better detection rate compared to the other planar antenna array configurations studied in this paper. Besides it outperforms another 2-L shaped antenna array configuration that had already been presented in [20] but in which the 3 sub-arrays along the axes were taken into account independently for the estimation of the source azimuth and elevation DOA. The proposed results of this paper show that despite their possibly cumbersome design, 3D antenna arrays are of great interest in applications requiring an increased estimation and

doi: 10.1049/iet-map.2008.0234

resolution precision. For example, this can be found in the airborne emergency positioning problem as mentioned in [25].

6 References

[1] VAN VEEN B.D., BUCKLEY K.M.: 'Beamforming: a versatile approach to spatial filtering', *IEEE ASSP Mag.*, 1988, **5**, pp. 4–24

[2] SCHMIDT R.O.: 'Multiple emitter location and signal parameter estimation', *IEEE Trans. Antennas Propag.*, 1986, **AP-34**, pp. 276–280

[3] PAULRAJ A., ROY R., KAILATH T.: 'A subspace rotation approach to signal parameter estimation', *Proc. IEEE*, 1986, **74**, pp. 1044–1045

[4] ROY R., KAILATH T.: 'ESPRIT—estimation of signal parameters via rotational invariance techniques', *IEEE Trans. Acoust. Speech Signal Process.*, 1989, **37**, (7), pp. 984–995

[5] ÇEKLI E., ÇIRPAN H.A.: 'Unconditional maximum likelihood approach for localization of near-field sources: analysis and performance analysis', *AEÜ Int. J. Electron. Commun.*, 2003, **57**, (1), pp. 9–15

[6] ZISKIND I., WAX M.: 'Maximum likelihood localization of multiple sources by alternating projection', *IEEE Trans. Acoust. Speech Signal Process.*, 1998, **36**, (10), pp. 1553–1560

[7] MOON T.K.: 'The expectation-maximization algorithm', *IEEE Signal Process. Mag.*, 1996, **13**, pp. 47–60

[8] ÇEKLI E., ÇIRPAN H.A.: 'Deterministic maximum likelihood approach for localisation of near-field sources', *AEÜ Int. J. Electron. Commun.*, 2002, **56**, (1), pp. 1–10

[9] KRIM J., VIBERG M.: 'Two decades of array signal processing research: the parametric approach', *IEEE Signal Process. Mag.*, 1996, **13**, pp. 67–94

[10] YANXING Z., QINYE Y.: 'Closed-form space-time channel blind estimation for space-time coded MC-CDMA systems', *IEICE Trans. Commun.*, 2005, **88**, (7), pp. 3050–3056

[11] WILSON P., PAPAZIAN P.: 'PCS band direction-of-arrival measurements using a 4 element linear array'. Vehicular Technology Conf., IEEE VTS-Fall VTC, September 2000, pp. 786–790

[12] VERTATSCHITSCH E.J., HAYKIN S.: 'Impact of linear array geometry on direction-of-arrival estimation for a single source', *IEEE Trans. Antennas Propag.*, 1991, **39**, pp. 576–584

[13] XU X., YE Z., ZHANG Y., CHANG C.: 'A deflation approach to direction of arrival estimation for symmetric uniform linear array', *IEEE Antennas Wirel. Propag. Lett.*, 2006, **5**, pp. 486–489

[14] LIANG J.W., PAULRAJ A.J.: 'On optimizing base station array topology for coverage extension in cellular radio networks'. 45th IEEE Vehicular Technology Conf., 1995, pp. 866–870

[15] ULKU B., RANDOLPH L.M.: 'On the geometry of isotropic arrays', *IEEE Trans. Signal Process.*, 2003, **51**, (6), pp. 1469–1478

[16] GAZZAH H., MARCOS S.: 'Cramer–Rao bounds for antenna array design', *IEEE Trans. Signal Process.*, 2006, **54**, (1), pp. 336–345

[17] LIANG J.-W., PAULRAJ A.J.: 'On optimizing base station antenna array topology for coverage extension in cellular radio networks'. IEEE 45th Vehicular Technology Conf., Stanford, CA, 1995, vol. 2, pp. 866–870

[18] HUA Y., SARKAR T.K., WEINER D.D.: 'An L shaped array for estimating 2-D directions of wave arrival', *IEEE Trans. Antennas Propag.*, 1991, **39**, pp. 143–146

[19] MANIKAS A., ALEXIOU A., KARIMI H.R.: 'Comparison of the ultimate direction-finding capabilities of a number of planar array geometries', *IEE Proc. Radar Sonar Navig.*, 1997, **144**, (6), pp. 321–329

[20] TAYEM N., KWON H.M.: 'L Shape 2-dimensional arrival angle estimation with propagator method', *IEEE Trans. Antennas Propag.*, 2005, **53**, pp. 1622–1630

[21] MAOHUI X.: 'New method of effective array for 2-D direction of arrival estimation', *Int. J. Innov. Comput. Inf. Control*, 2006, **2**, pp. 1391–1397

[22] WONG K.T., LI L., ZOLTOWSKI M.D.: 'Root-MUSIC-based direction-finding and polarization estimation using diversely polarized possibly collocated antennas', *IEEE Antennas Propag. Lett.*, 2004, **3**, pp. 129–132

[23] SALAMEH A., TAYEM N., KWON H.M.: 'Improved 2-D root MUSIC for non-circular signals'. Proc. IEEE Sensor Array and Multichannel Signal Processing Workshop, 12 July 2006, pp. 151–156

[24] VAN TRESS H.L.: 'Detection, estimation and modulation theory, part I' (Wiley, New York, 1968)

[25] GAZZAH H., MARCOS S.: 'Directive antenna arrays for 3D source localization'. Proc. 4th IEEE Workshop on Signal Processing Advances in Wireless Communications (SPAWC), Florence, 15–18 June 2003